



Trans. Nonferrous Met. Soc. China 22(2012) 1250-1254

Transactions of Nonferrous Metals Society of China

www.tnmsc.cn

Electrochemical oxidation behavior of pyrite bioleaching by *Acidthiobacillus ferrooxidans*

GU Guo-hua¹, SUN Xiao-jun^{1,2}, HU Ke-ting¹, LI Jian-hua^{1,2}, QIU Guan-zhou¹

- 1. School of Minerals Processing and Bioengineering, Central South University, Changsha 410083, China;
 - 2. Daye Nonferrous Metal Group Design & Research Institute Company, Ltd., Huangshi 435005, China

Received 9 May 2011; accepted 30 August 2011

Abstract: The electrochemical oxidation behavior of pyrite in bioleaching system of *Acidthiobacillus ferrooxidans* was investigated by cyclic voltammetry (CV), polarization curve and electrochemical impedance spectroscopy (EIS). The results show that in the presence or absence of *A. ferrooxidans*, the oxidation reaction of pyrite is divided into two steps: the first reaction step involves the oxidation of pyrite to S, and the second reaction step is the oxidation of S to SO_4^{2-} . The oxidation mechanism of pyrite is not changed in the presence of *A. ferrooxidans*, but the oxidation rate of pyrite is accelerated. With the extension of reaction time of *A. ferrooxidan* with pyrite, the polarization current density of pyrite increases and the breakdown potential at which the passive film dissolves decreases. The impedance in the presence of *A. ferrooxidans* is obviously lower than that in the absence of *A. ferrooxidans*, further indicating that microorganism accelerates the corrosion process of pyrite.

Key words: pyrite; bioleaching; A. ferrooxidans; electrochemistry

1 Introduction

As a processing technique for sulfide ores, bioleaching is expanding rapidly. Pyrite is the most common sulfide mineral in nature. A better understanding of the reactivity and oxidation of pyrite in bioleaching process is needed for improving the rate of dissolution of valuable metals from ores.

The dissolution of pyrite in bioleaching system is a complex electrochemical process with electron transfer. Electron transfer among mineral surface, interface of bacteria and leaching solution is the root cause of the oxidation–reduction reaction. It is feasible to investigate and analyze the electrochemical oxidation behavior of pyrite in bio-leaching system of *Acidthiobacillus ferrooxidans* by electrochemical theory and methods [1,2]. Electrochemical methods can convert chemical value that is generally difficult to measure to electrochemical parameters [3–5]. LIU et al [6–8] researched the electrochemical behavior of hydrothermal and sedimentary pyrite in acidic solution and found that the dissolution of pyrite was related to potential. Pyrite was oxidized to S below 0.6 V (vs SCE) and the

oxidation rate was very slow; above 0.6 V (vs SCE), the oxidation rate increased. They also pointed out that the rate of pyrite dissolution was weakly dependent on the solution pH. While PASCHKA and DZOMBAK [9] argued that the rate of pyrite oxidation increased with the increase of concentration of Fe³⁺ ions and dissolved O₂, and decreased with the increase of concentrations of Fe²⁺ and H⁺ ions in the solution. CHERMYSHOVA [10] studied the pyrite oxidative dissolution products, and held that the reaction products were found to vary with applied potential, electrolyte composition and solution pH. HOMES and CRUNDWELL [11] used the electrochemical approach to examine the kinetics of pyrite oxidation and derived the rate expression of pyrite oxidation. These studies [6-11] focused on pyrite oxidative dissolution products under various aqueous conditions. SO_4^{2-} , $Fe(OH)_3(s)$, Fe^{2+} and Fe^{3+} have been identified as the reaction products in aqueous solutions, with elemental S and other polysulfides as intermediates on the pyrite electrode surface.

As it is known, microorganisms are important in metal recovery from pyrite. *A. ferrooxidan* is the most important iron- and sulfur-oxidizing bacteria [12,13]. However, there are a few detailed reports about utilizing

electrochemical measurements for studying the oxidation mechanism of pyrite with bacterial involvement [14]. In this work, cyclic voltammetry (CV), polarization curve and electrochemical impedance spectroscopy were used to investigate the electrochemical behavior of pyrite in the presence and absence of *A. ferrooxidans*, and to improve the understanding of the reaction mechanisms involved in the pyrite electrobioleaching.

2 Experimental

2.1 Microorganisms and culture media

The strain of *A. ferrooxidans* (ATCC23270) used in the experiment was conserved by the Key Laboratory of Biometallurgy in Central South University, China. Before the experiment, *A. ferrooxidans* were cultured in 9K medium replacing the ferrous sulfate with 4% FeS₂ as the sole energy source at 30 °C and initial pH 2.0. The 9K medium contained 3.0 g/L (NH₄)₂SO₄, 0.1 g/L KCl, 0.5 g/L K₂HPO₄, 0.5 g/L MgSO₄·7H₂O, 0.01 g/L Ca(NO₃)₂. When the bacteria reached the logarithmic growth period, cells were harvested by centrifugation and washed twice with electrolyte. The concentration of strains used in the experiments was 1×10⁸ cell/mL.

2.2 Mineral and electrode

The sample of pyrite used in this study was obtained from Yunfu Sulfur Iron Ore, Guangdong Province, China. Pyrite sample with fine crystallization was selected as the working electrode, and was cut into $d12 \text{ mm} \times 4 \text{ mm}$ cylinder. The cylinder was put into specially designed electrode sets and only one side was exposed. The effective area of pyrite electrode was 1 cm^2 .

2.3 Electrochemical experiment

The electrochemical measurements were performed using a three-electrode arrangement with a working electrode (pyrite), a graphite rod as auxiliary electrode and an $Ag|AgCl|KCl_{sat}$ reference electrode. The electrolyte was 9K and 0.1 mol/L Na₂SO₄ solution. The solution pH was adjusted to 2.0 with H₂SO₄. All reagents were analytical grade products. Distilled water was used in experiment. The three electrodes and the electrolyte were placed in a water thermostat system, which was kept at constant temperature. All potentials were referenced to the saturated calomel electrode (SCE). The solid pyrite electrode was prepared by sequentially polishing with 300, 500 and 600 grades silicon carbide paper. After polishing, the electrode was rinsed with ethanol and distilled water. A Princeton Potentiostat/ Galvanostat 273&Lock-in Amplifer produced by EG&G Princeton Applied Research Corp., USA, was used to perform the electrochemical measurements.

3 Results and discussion

3.1 Polarization curves of pyrite

Figure 1 shows the polarization curves of pyrite in the presence and absence of A. ferrooxidans. Before the measurement, electrodes were soaked in the electrolyte for 30 min. It can be seen from Fig. 1 that when the applied potential swept from point a to point b, no current signals appeared. This implies that the surface of electrode was passivated in the initial stage of scanning. When the applied potential swept over point b, the current density increased rapidly because the passive film was broken up. The potential and current density at point b are the pitting potential and pitting current density of the pyrite electrode.

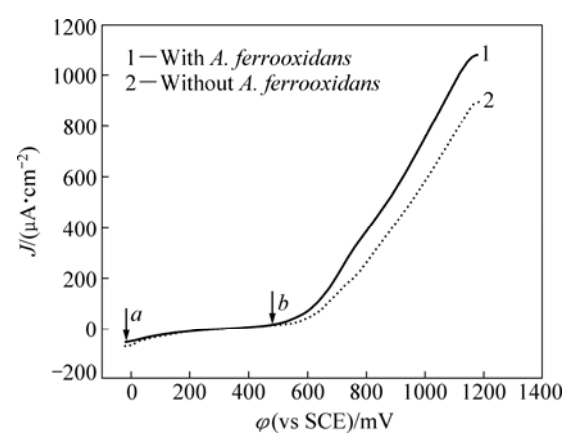


Fig. 1 Polarization curves of pyrite in the presence and absence of *A. ferrooxidans* (pH=2.0; t=30 °C; scan rate 1 mV/s)

Figure 1 also shows that the pitting potential and pitting current density of the pyrite electrode have no significant difference with or without bacteria involvement. But the polarization current density of pyrite in the leaching system with *A. ferrooxidans* was higher than that in the sterile solution after the potential reaches the pitting potential. That is to say, the corrosion rate of pyrite was accelerated by *A. ferrooxidan*.

3.2 Cyclic voltammetry of pyrite electrode

Cyclic voltammogram obtained from pyrite electrode is shown in Fig. 2. Before the experiment, the pyrite electrodes were immersed in the electrolyte for 30 min. The results indicate that in the electrode potential region of -0.6 to 0.8 V (vs SCE), in the sterile solution, the polarization current density of pyrite was small. Above 0.6 V (vs SCE), the current density increased. These results can be explained by the two-step oxidation reaction model proposed by LIN and SAY [15]. Pyrite is firstly oxidized to S by reaction (1), which makes the electrode passivated; above 0.6 V (vs SCE), S is oxidized to SO_4^{2-} by reaction (2) and the passive film is broken

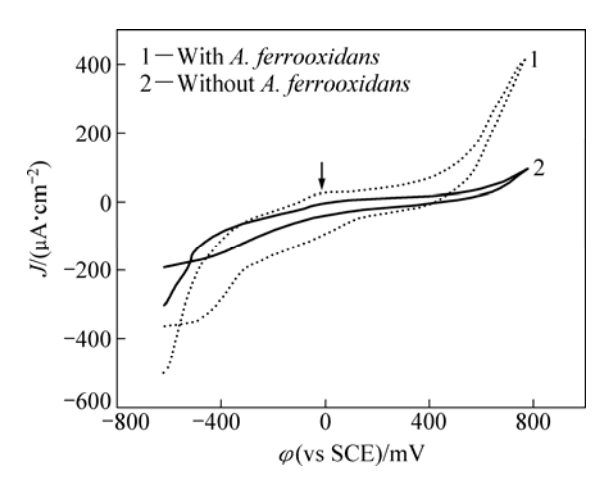


Fig. 2 Cyclic voltammetry curves of pyrite in the presence and absence of *A. ferrooxidans* (pH=2.0; *t*=30 °C; scan rate 20 mV/s)

up. Although in this study there is no distinguishable oxidation peak below 0.6 V (vs SCE) for S film formation, the results of polarization curves and the relatively high current density beyond 0.6 (vs SCE) are suggestive of oxidation of a surface film formed at lower potentials, and which is consistent with other studies [6].

$$FeS_2 \rightarrow Fe^{2+} + 2S + 2e \tag{1}$$

$$FeS_2 + 8H_2O \rightarrow 2SO_4^{2-} + Fe^{3+} + 16H^+ + 15e$$
 (2)

In the leaching solution with *A. ferrooxidans*, a weak oxidation peak was observed around 0 V (vs SCE), indicating S film formation. And it can be seen that the oxidation of the S film on the pyrite surface occurred at a lower oxidation potential than in the sterile solution, and the oxidation current of pyrite was obviously increased. These results in the presence and absence of *A. ferrooxidans* show that the process of pyrite oxidation was not changed, but the oxidation rate of pyrite was accelerated by *A. ferrooxidans*.

During reverse scanning process of cathode, a reduction peak around -0.5 V (vs SCE) was observed. It could be interpreted as two possible reactions: 1) the reduction of S formed electrochemically during the oxidation scan, and 2) the reduction of FeS₂(s) to form FeS(s) and H₂S.

Cyclic voltammograms obtained during the reaction of pyrite electrode at different time are shown in Fig. 3. Prior to tests, electrodes were interacted with *A. ferrooxidan* solution for 5 min, 3 d and 9 d, respectively. It can be seen that within the electrode potential region of –0.6 to 0.8 V (vs SCE), there was a passivation region in the curve during the anodic scanning process. This was probably caused by the oxidation reaction by which pyrite was oxidized to S, and then the electrode was passivated. As the potential rose, the passive film dissolved and the current density increased rapidly.

Comparing the curves at different reaction time of *A. ferrooxidan* with pyrite in Fig. 3, it is found that, the longer the interaction time, the greater the polarization current density of the pyrite, and the lower the breakdown potential at which the passive film dissolved. In conclusion, the corrosion rate of pyrite increased after the reaction of *A. ferrooxidan* with pyrite.

3.3 Electrochemical impedance spectroscopy of pyrite

Figure 4 illustrates the electrochemical impedance

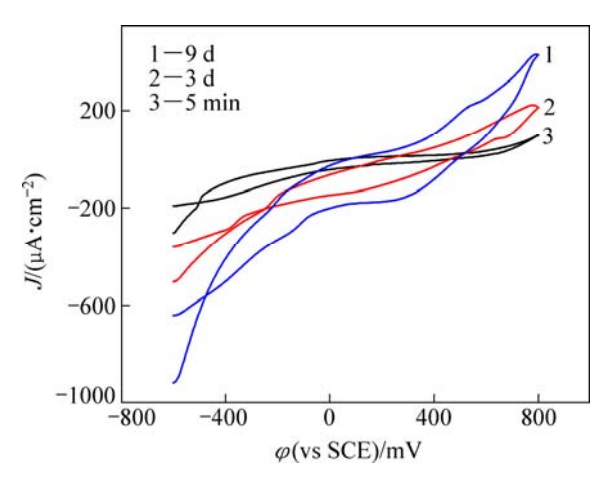


Fig. 3 Cyclic voltammetry curves of pyrite electrode in the presence of *A. ferrooxidans* at different interaction time (pH=2.0; *t*=30 °C; scan rate 20 mV/s; 9K+0.1 mol/L Na₂SO₄)

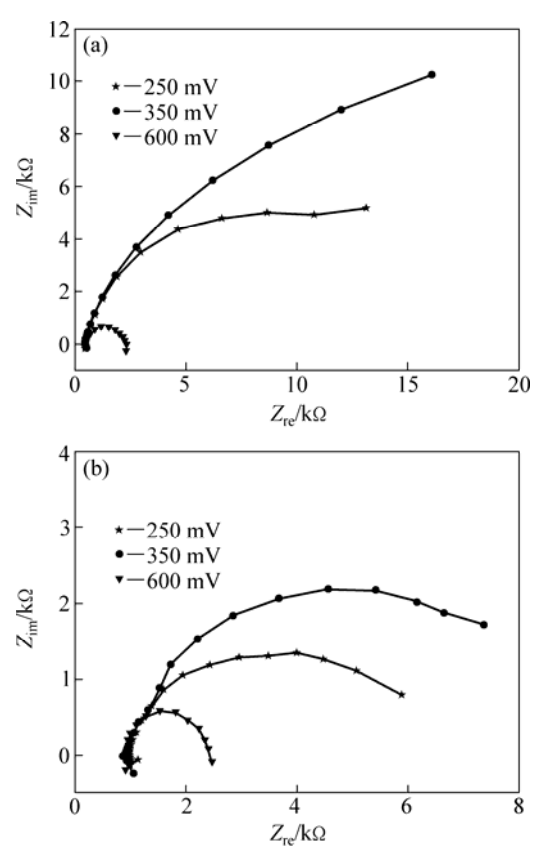


Fig. 4 EIS of pyrite in the absence (a) and presence (b) of *A. ferrooxidans* (t=30 °C; pH=2.0; f=10⁻²-10⁵Hz)

spectroscopy (EIS) of pyrite electrode in the presence and absence of *A. ferrooxidans*. The capacitive components were observed from the impedance loops. But at different potentials, the reaction on the surface of pyrite was not the same.

As the anodic polarization potential increased, a significant increase was seen in the loops below 0.35 V (vs SCE). It showed that pyrite was dissolved partially and elemental sulfur was produced. Passive sulfur film formed and anodic reaction was hindered. The process was the growth of passive film. The equivalent circuit shown in Fig. 5(a) was proposed for fitting EIS diagrams and was applied below 0.35 V (vs SCE). In Fig. 5(a), the R_{Ω} represents the solution resistance; $R_{\rm p}$ is associated with the charge transfer resistance; CPE1 is the constant phase element which represents the diffusion impedance of reaction products; CPE2 is the constant phase element which substitutes the capacitor of the double-layer. At 0.6 V (vs SCE), the loop decreased. It proved that the passive film formed below 0.35 V (vs SCE) was dissolved. The equivalent circuit at this stage is shown in Fig. 5(b). The results are consistent with the cyclic voltammograms at corresponding potential. Figure 6 shows the measured values of EIS and the corresponding analog values of pyrite in the presence and absence of A. ferrooxidans at 0.35 V and 0.6 V. It can be seen that the equivalent circuit agreed fairly well with electrochemical impedance spectroscopy, which indicated that the proposed equivalent circuit can well reflect the electrochemistry behavior of pyrite.

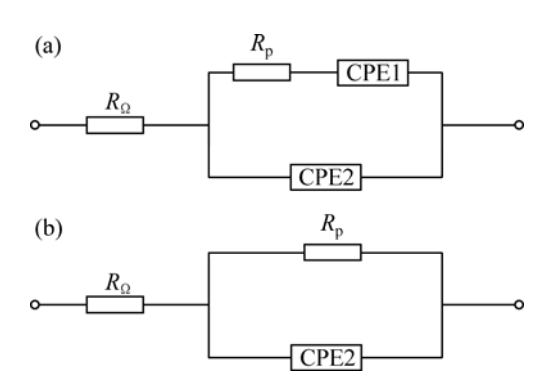


Fig. 5 Equivalent circuit for pyrite in the presence and absence of *A. ferrooxidans*: (a) Between 0.15-0.35 V; (b) Between 0.35-0.60 V

Figure 4 also indicates that the electrochemical impedance spectroscopy of pyrite with or without *A. ferrooxidans* involvement was similar. But the impedance with *A. ferrooxidans* was much lower than that without. The bacteria removed the passive film on pyrite surface or inhibited its formation, reducing the impedance and accelerating the dissolution rate of pyrite.

In Fig. 7, the EIS of pyrite as a function of reaction time of *A. ferrooxidans* shows an arc at high frequency

and an oblique line at low frequency. This proved that oxidation reaction was controlled by electron transfer step at high frequency and was diffusion controlled at low frequency. The resistance of electron transfer firstly increased and then decreased. After 9 d, the electrode surface was covered by yellow substance, which may be jarosite; after 12 d, the amount of yellow substance increased. From Fig. 6, it is deduced that after pyrite was oxidized by *A. ferrooxidans*, the resistance of pyrite

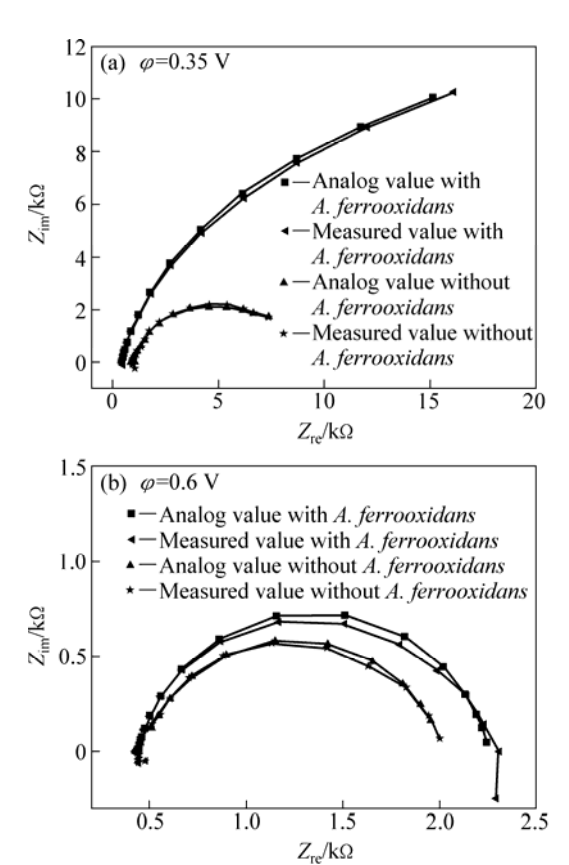


Fig. 6 EIS and corresponding analog values of pyrite in the presence and absence of *A. ferrooxidans* at 0.35 V (a) and 0.6 V (b)

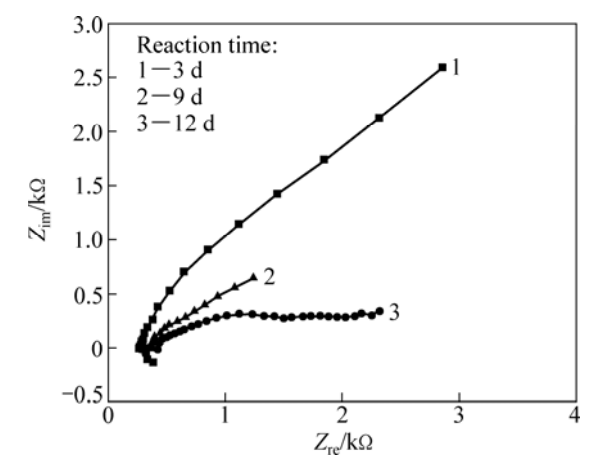


Fig. 7 EIS of pyrite as function of reaction time of *A. ferrooxidans* and pyrite (t=30 °C; pH=2.0; φ =450 mV; f=10⁻²-10⁵ Hz; 9K+0.1 mol/L Na₂SO₄)

oxidation firstly decreased and then increased because jarosite covered the electrode surface.

4 Conclusions

- 1) Cyclic voltammetry curve shows that in the presence or absence of *A. ferrooxidans*, pyrite is firstly oxidized to S, which makes electrode passivated; above 0.6 V (vs SCE), S is oxidized to SO₄²⁻. The polarization current density of pyrite and the oxidation rate of pyrite are accelerated by *A. ferrooxidans*.
- 2) The electrochemical impedance spectroscopy indicates that the reactions on the surface of pyrite are not the same at different potentials. Pyrite is oxidized and produces passive film at 0.25 V–0.35 V (vs SCE); but above 0.6 V (vs SCE), passive film is dissolved and the impedance decreases. The electrochemical impedance spectroscopy of pyrite with or without *A. ferrooxidans* involvement is similar. However, the impedance with *A. ferrooxidans* is much lower than that without *A. ferrooxidans*.

References

- [1] LI Hai-bo, CAO Hong-bin, ZHANG Guang-ji, ZHANG Yi, FANG Zhao-heng. A review on bioleaching mechanism and electrochemistry of arsenic-bearing gold ores [J]. The Chinese Journal of Process Engineering, 2006, 6(5): 849–856. (in Chinese)
- [2] TAO Xiu-xiang, GONG Guan-qun, LIU Jin-yan, MEI Jian, CHEN Zeng-qiang, CHEN Jian-zhong. Electrochemical mechanism of coal biodesulphurization [J]. Journal of China University of Mining and Technology, 2007, 36(4): 431–435. (in Chinese)
- [3] LI Hong-xu, WANG Dian-zuo. Electrochemistry of sulfide bio-leaching (I) [J]. Mining and Metallurgy, 2002, 11(4): 49-53. (in

Chinese)

- [4] ZHU Li, ZHANG De-cheng, LUO Xue-gang. Electrochemical behavior of chalcopyrite in sulfuric acid leaching [J]. Metal Mine, 2008(5): 66–70. (in Chinese)
- [5] YU Run-lan, QIU Guan-zhou, HU Yue-hua. Difference in electrochemical behavior between marmatite and pyrrhotite in Ca(OH)₂ system [J]. Metal Mine, 2005(8): 30–33. (in Chinese)
- [6] LIU R, WOLFE A L, DZOMBAK D A, HORWITZ C P, STEWART B W. Electrochemical study of hydrothermal and sedimentary pyrite dissolution [J]. Applied Geochemistry, 2008, 23: 2724–2734.
- [7] LIU R, WOLFE A L, DZOMBAK D A, HORWITZ C P, STEWART B W. Controlled electrochemical dissolution of hydrothermal and sedimentary pyrite [J]. Applied Geochemistry, 2009, 24: 836–842.
- [8] LIU R, WOLFE A L, DZOMBAK D A, HORWITZ C P, STEWART B W. Comparison of dissolution under oxic acid drainage conditions for eight sedimentary and hydrothermal pyrite samples [J]. Environmental Geology, 2008, 56(1): 171–182.
- [9] PASCHKA M G, DZOMBAK D A. Use of dissolved sulfur species to measure pyrite dissolution in water at pH 3 and 6 [J]. Environmental Engineering Science, 2004, 21: 411–420.
- [10] CHEMYSHOVA I V. Pyrite oxidation mechanism in aqueous solutions: An in situ FTIR study [J]. Russ J Appl Electrochem, 2004, 40: 69-77.
- [11] HOLMES P R, CRUNDELL F K. The kinetics of the oxidation of pyrite by ferric ions and dissolved oxygen: An electrochemical study [J]. Geochim Cosmochim Acta, 2000, 64: 263–274.
- [12] LIU Jian-she. Bioextraction and corrosion electrochemistry of sulfide minerals [D]. Changsha: Central South University, 2002. (in Chinese)
- [13] LI Hong-xu. Copper sulfide bio-metallurgy [M]. Beijing: Metallurgical Industry Press, 2007. (in Chinese)
- [14] CABRAL T, IGNATIADIS I. Mechanistic study of the pyrite-solution interface during the oxidative bacterial dissolution of pyrite (FeS₂) by using electrochemical techniques [J]. International Journal of Mineral Processing, 2001, 62: 41–64.
- [15] LIN H K, SAY W C. Study of pyrite oxidation by cyclic voltammetric, impedance spectroscopic and potential step techniques [J]. Journal of Applied Electrochemistry, 1999, 29: 987–994.

氧化亚铁硫杆菌浸矿体系中黄铁矿的电化学行为

顾帼华1, 孙小俊1,2, 胡可婷1, 李建华1,2, 邱冠周1

- 1. 中南大学 资源加工与生物工程学院,长沙 410083;
 - 2. 大冶有色设计研究院有限公司, 黄石 435005

摘 要:运用循环伏安、稳态极化扫描和交流阻抗等电化学测试方法,研究黄铁矿在氧化亚铁硫杆菌浸矿体系和无菌酸性体系下的电化学氧化机理。结果表明,在无菌和 A. ferrooxidans 菌存在的条件下,黄铁矿的氧化反应分为两步:第一步是黄铁矿氧化生成元素 S;第二步是元素 S被氧化生成 SO_4^{2-} 。加入 A. ferrooxidans 后黄铁矿的氧化机理没有发生改变,但是氧化速度加快。随着黄铁矿与 A. ferrooxidans 作用时间的延长,极化电流密度增加,黄铁矿表面钝化膜溶解的点蚀电位降低。在细菌存在的条件下,电极的阻抗值下降,表明微生物的存在加速了黄铁矿电极的腐蚀作用,有利于黄铁矿的氧化溶解。

关键词: 黄铁矿; 生物浸出; 氧化亚铁硫杆菌; 电化学